Simultaneous fluorescence and quantitative phase microscopy with single-pixel detectors

Yang Liu[a], Jinli Suo[a], Yuanlong Zhang[a], and Qionghai Dai[a,*]

[a]Department of Automation, Tsinghua University, Beijing 100084, China.

ABSTRACT

Multimodal microscopy offers high flexibilities for biomedical observation and diagnosis. Conventional multimodal approaches either use multiple cameras or a single camera spatially multiplexing different modes. The former needs expertise demanding alignment and the latter suffers from limited spatial resolution. Here, we report an alignment-free full-resolution simultaneous fluorescence and quantitative phase imaging approach using single-pixel detectors. By combining reference-free interferometry with single-pixel detection, we encode the phase and fluorescence of the sample in two detection arms at the same time. Then we employ structured illumination and the correlated measurements between the sample and the illuminations for reconstruction. The recovered fluorescence and phase images are inherently aligned thanks to single-pixel detection. To validate the proposed method, we built a proof-of-concept setup for first imaging the phase of etched glass with the depth of a few hundred nanometers and then imaging the fluorescence and phase of the quantum dot drop. This method holds great potential for multispectral fluorescence microscopy with additional single-pixel detectors or a spectrometer. Besides, this cost-efficient multimodal system might find broad applications in biomedical science and neuroscience.

Keywords: Multimodal microscopy, Quantitative phase imaging, Fluorescence microscopy, Single-pixel imaging

1. INTRODUCTION

Fluorescence microscopy serves as a powerful tool for biomedical observation and diagnosis, especially when combined with confocal and two-photon techniques.[1] By probing the proteins or other molecules with fluorescent stains, one could monitor the physiological state of the specimens, including live cells, which provides functional information for biomedical imaging. However, fluorescence microscopy generally lacks the structural information of the specimens. Because most thin specimens do not absorb or scatter light significantly, that is they are transparent or translucent, so the morphological information is lost in fluorescence detection.[2] Quantitative phase imaging is an emerging technique for structural characterization of transparent specimens quantitatively. The combination of fluorescence and phase imaging would provide both the functional and structural features for more accurate and flexible observation and diagnosis in a wide range of fields, from basic science to clinical applications.

Conventional methods for simultaneous fluorescence and phase imaging either use multiple well-aligned cameras or a single camera with spatial multiplexing.[3,4] The former needs expertise demanding alignment and the latter trades off spatial resolution for multiple capture modes.[5] However, single-pixel imaging offers an alternative solution for alignment-free, full-resolution multimodal imaging. By exploiting structured illumination and sequential correlated measurements between the sample and the illuminations, one could recover the original two-dimensional (2D) information of the sample computationally and compressively.[6]

Here, we report an alignment-free full-resolution simultaneous fluorescence and quantitative phase imaging approach using two single-pixel detectors. Single-pixel imaging has been applied for dual- or multiple- modality tasks thanks to the high-sensitivity, wide-spectrum-range and low-cost property of single-pixel detectors. Recent advances include four angles of illumination for three-dimensional imaging,[7] dual wavelengths for infrared

* Further author information: (Send correspondence to Q.D.)
Q.D.: E-mail: qhdai@tsinghua.edu.cn

Quantitative Phase Imaging IV, edited by Gabriel Popescu, YongKeun Park,
Proc. of SPIE Vol. 10503, 105032K · © 2018 SPIE · CCC code:
1605-7422/18/$18 · doi: 10.1117/12.2286757

and visible imaging,[8,9] and multiple-wavelength illumination for color or multispectral imaging.[10–14] However, simultaneous fluorescence and quantitative phase imaging using single-pixel detectors has not been reported yet, to the best of our knowledge.

Previous single-pixel phase imaging method generally requires phase-mode spatial light modulation and two-beam interferometry.[15–17] However, phase-mode spatial light modulation is relatively slow with a typical refreshing rate of 60 Hz, which limits the acquisition time to a few minutes. Recently, González et al. used the high-speed binary amplitude modulator, i.e., the digital micromirror device (DMD) for phase modulation[18] and obtained single-pixel digital holography within a few seconds.[19] However, these two-beam interferometry methods suffer from phase stability issues,[17] since single-pixel imaging requires thousands of sequential measurements and the corrupted phases would damage the reconstruction. Recently, a reference-free approach for single-pixel phase imaging has been demonstrated using the DMD for complex amplitude modualtion[20] to form a common-path reference beam with single-point detection.[21] However, it lacks the ability of simultaneous fluorescence imaging because of its passive imaging modality.

By combining reference-free interferometry with single-pixel detection, we encode the phase and fluorescence of the sample in two detection arms at the same time. We employ active imaging, i.e., complex structured illumination and add a bucket detector for fluorescence imaging to achieve simultaneous fluorescence and phase imaging. It is worth noting that these two modes are conducted in a parallel manner and do not require expertise demanding alignment of multiple cameras. Moreover, this method holds great potential for multispectral fluorescence microscopy with additional single-pixel detectors or a spectrometer.[10–13] We further envision that this cost-efficient multimodal system might find broad applications in biomedical science and neuroscience.

2. SINGLE-PIXEL PHASE AND FLUORESCENCE IMAGING

Single-pixel imaging or the single-pixel camera[6] illuminates the sample with structured light and measures the integrated intensity of the sample illuminated by structured light with a single-pixel detector. The transmission or reflection intensity of the sample can be recovered with multiple sequential illuminations and measurements.

In this section, we introduce the single-pixel phase and fluorescence imaging method. First, we briefly summarize the forward model of single-pixel imaging and the reconstruction method. Then, we introduce the single-pixel imaging method using reference-free phase-shifting interferometry and complex amplitude modulation. Finally, we show that the phase-shifting patterns can be used for fluorescence imaging at the same time.

2.1 Single-pixel Imaging

For a 2D sample with complex field $S(\vec{r})$ illuminated by a spatially modualted pattern $P_k(\vec{r})$, where k is the index of the pattern ($k = 1, \cdots, M$) and $\vec{r}$ is the spatial vector, the measured intensity can be expressed as

$$I_k = \iint_{\Omega} |P_k(\vec{r}) \cdot S(\vec{r})|^2 \, \mathrm{d}^2\vec{r} = \iint_{\Omega} |P_k(\vec{r})|^2 \cdot |S(\vec{r})|^2 \, \mathrm{d}^2\vec{r}, \tag{1}$$

where $\iint_{\Omega} \cdot \, \mathrm{d}^2\vec{r}$ denotes integration over the 2D region of interest Ω. The intensity can be rewritten as the discreted version

$$I_k = \sum_{(i,j)} P_k \circ S \,, \tag{2}$$

where $\circ$ denotes element-wise product or Hadamard product, $P_k(i,j)$ and $S(i,j)$ is the discreted field of $|P_k(\vec{r})|^2$ and $|S(\vec{r})|^2$ ($i = 1, \cdots, m,\ j = 1, \cdots, n,\ N = m \cdot n$), and $\sum_{(i,j)}$ denotes the sum of the whole 2D matrix with subindex (i,j). After vectorization of the sample field and the illumination field, the forward model of single-pixel imaging can be expressed as a linear model

$$\boldsymbol{I} = \boldsymbol{P} \cdot \boldsymbol{S} \,, \tag{3}$$

where $\boldsymbol{S} \in \mathbb{C}^N$ is the vectorized sample field $S(i,j)$, $\boldsymbol{P} \in \mathbb{C}^{M \times N}$ is the row-wise rearrangement of the vectorized illumination field $P_k(i,j)$ for each k, and $\boldsymbol{I} \in \mathbb{C}^M$ is the colomn-wise rearrangement of each measurements I_k. If the measurement matrix or sensing matrix $\boldsymbol{P}$ is the full orthonormal bases, such as the Fourier transform

bases[22] or Walsh-Hadamard transform bases,[23] the sample field can be reconstructed via the corresponding inverse transform

$$\boldsymbol{S} = \boldsymbol{P}^{-1} \cdot \boldsymbol{I}\,. \tag{4}$$

If the measurements are over-sampled, Moore-Penrose inverse or pseudoinverse can be applied for reconstruction. If under-sampled, compressive sensing methods based on the assumption that most natural scenes are inherently sparse under specific domain can be used for reliable recovery.[24,25] In this work, we utilize basis transform for simplicity.

2.2 Single-pixel Phase Imaging

We use the reference-free method for single-pixel phase imaging, which is firstly reported by Ref. 21. We adapt the passive imaging scheme to active imaging mode to obtain the fluorescence information of the sample at the same time.

The forward model is different from conventional single-pixel imaging, since the original total-intensity measurements would wash out the phase information induced both by the sample and the structured illuminations. For single-pixel phase imaging, we measure the single-point intensity at the center of the Fourier plane of the correlated field between the sample and the illuminations. The single-point intensity can be expressed as

$$I_k = \left|\left(P_k(\vec{r}) \circ S(\vec{r})\right)_{\vec{k}=0}\right|^2 = \left|\iint\limits_{\Omega} P_k(\vec{r}) \cdot S(\vec{r})\,\mathrm{d}^2\vec{r}\right|^2, \tag{5}$$

where $\vec{k}$ denotes the spatial frequency vector and $\vec{k} = 0$ represents the center point of the Fourier plane. In this way, the phase of both sample and illuminations is preserved. By introducing a reference beam and phase shifts in the complex structured illumination, that is $P_{k,\phi} = (\mathrm{e}^{\mathrm{j}\phi} \cdot H_k + 1)/2$, where H_k is one basis of Walsh-Hadamard transform consisting of $\{+1, -1\}$ elements. The single-point intensity can be rewritten as phase-shifting interferometry form

$$\begin{aligned} I_{k,\phi} &= \left|\iint\limits_{\Omega} \frac{1}{2}[\mathrm{e}^{\mathrm{j}\phi} H_k(\vec{r}) + 1] \cdot S(\vec{r})\,\mathrm{d}^2\vec{r}\right|^2 = \frac{1}{4}\left|\mathrm{e}^{\mathrm{j}\phi} \cdot \iint\limits_{\Omega} H_k(\vec{r}) S(\vec{r})\,\mathrm{d}^2\vec{r} + \iint\limits_{\Omega} S(\vec{r})\,\mathrm{d}^2\vec{r}\right|^2 \\ &= \frac{1}{4}\left|\mathrm{e}^{\mathrm{j}\phi} \cdot s_k + r\right|^2 \end{aligned} \tag{6}$$

where $s_k = \iint_{\Omega} H_k(\vec{r}) S(\vec{r})\,\mathrm{d}^2\vec{r}$ is the integration of the complex field of the sample coded by the illumination, $r = \iint_{\Omega} S(\vec{r})\,\mathrm{d}^2\vec{r}$ is a constant, which is referred as the reference beam for the interferometry. With three-step phase-shifting, that is $\phi = 0, \pi/2, \pi$, the complex integration can be recovered by

$$y_k = (I_{k,0} - I_{k,\pi}) + \mathrm{j}(2I_{k,\pi/2} - I_{k,0} - I_{k,\pi}) = s_k \cdot r^* = r^* \cdot \iint_{\Omega} H_k(\vec{r}) S(\vec{r})\,\mathrm{d}^2\vec{r}. \tag{7}$$

In this way, the complex amplitude of the complex integration is recovered, and inverse Walsh-Hadamard transform can be applied to reconstruct the complex amplitude of the sample field as Eq. (4) shows. Thus, single-point detection enables single-pixel phase imaging.

2.3 Single-pixel Fluorescence Imaging

For fluorescence detection, total intensity of the fluorescence field is measured. Becasuse fluorescence light is incoherent, the forward model follows Eq. (1),

$$I^{\mathrm{F}}_{k,\phi} = \iint\limits_{\Omega} |P_{k,\phi}(\vec{r})|^2 \cdot F(\vec{r})\,\mathrm{d}^2\vec{r}, \tag{8}$$

where $F(\vec{r})$ denotes the fluorescence intensity of the sample.

Fluorescence detection can be conducted parallelly with phase detection by shared Walsh-Hadamard pattern illuminations. For $P_{k,\phi} = (\mathrm{e}^{\mathrm{j}\phi} \cdot H_k + 1)/2$, when $\phi = 0$ or π, all elements of $P_{k,\phi}$ are either 0 or 1, in this way

$$|P_{k,0}|^2 = P_{k,0} = (H_k + 1)/2\,, \quad \text{and} \quad |P_{k,\pi}|^2 = P_{k,\pi} = (-H_k + 1)/2\,. \tag{9}$$

Therefore, the fluorescence integration can be recovered with two phase shifts

$$y_k^{\mathrm{F}} = I_{k,0}^{\mathrm{F}} - I_{k,\pi}^{\mathrm{F}} = \iint\limits_{\Omega} H_k(\vec{r}) F(\vec{r})\, \mathrm{d}^2\vec{r} \tag{10}$$

Similarly, the fluoresence intensity can be recontructed via inverse Walsh-Hadamard transform as Eq. (4) shows. Note that Eq. (7) and Eq. (10) looks similar, but different in principle: Eq. (7) is based on phase-shifting interferometry, while Eq. (10) contains subtraction of two phase shifts because the elements of Walsh-Hadamard matrix are $+1$ and -1 and negative intensity can not be displayed on the binary spatial light modulator.

In sum, both the phase and fluorescence of the sample can be reconstructed simultaneously. Since the fluorescence detection arm only uses two of the three-step phase shifts, the total sequential measurements remain the same as the phase detection arm and fluorescence information can be acquired via total-intensity fluorescence detection.

3. EXPERIMENTAL SETUP

The scheme of the experimental setup is shown in Fig. 1. We use a single-frequency 488 nm laser source (Sapphire 488SF-100mW, Coherent) here. The incident light is expanded and collimated by a spatial filter, consisting of an objetive lens (OL_1), a pinhole, and a collimating lens (CL). The diameter of the output beam is around 20 mm to match the size of the DMD (Discovery 4100, Texas Instruments supplied by WinTech). The pixel resolution of the DMD is 1024×768 with pixel size of 13.68 µm. The DMD has a maximum refreshing rate of 20 kHz for binary patterns. A 4f system is applied to enable DMD with complex amplitude modulation using Lee hologram.[18] The 4f system consists of two lenses (L_1 and L_2) and a pinhole at the Fourier plane with a diameter of ∼0.8 mm, which directly blocks all other orders except the +1st order. The focal length of L_1 is 200 mm, and that of L_2 is chosen to match the lateral resolution and field of view of the sample. We use the focal length of 30 mm in the experiment to obtain $\sim 1.5 \times 1.5\,\mathrm{mm}^2$ field of view. Three of the patterns used in the experiment are shown in Fig. 1, where $0, \pi/2, \pi$ represents three phase shifts of the Walsh-Hadamard pattern and the insert is the cross part of the $\phi = \pi/2$ pattern containing phase difference between the left part and the right part. Then the desired complex amplitude field interacts with the sample field at the sample plane, which is conjugate with the DMD plane.

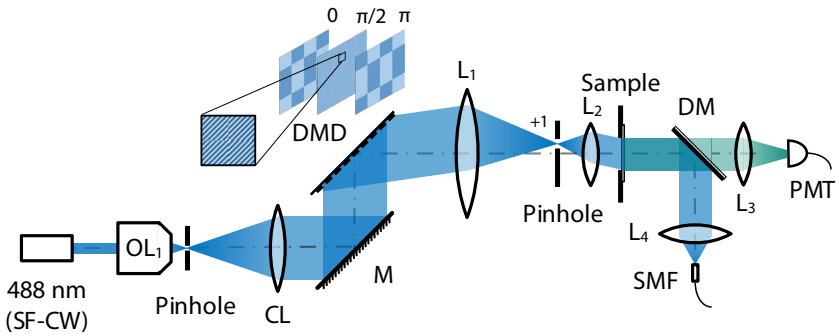

Figure 1. Experimental setup for simultaneous fluorescence and phase imaging with single-pixel detectors. Lee hologram[18] is applied for generating complex amplitude field at the sample plane, which provides both reference beam and phase shifts for interferometry. OL_1, objective lens; CL, collimating lens; M, mirror; DMD, digital micromirror device; L_1-L_4, lenses ($f_1 = 200$ mm, $f_2 = 30$ mm, $f_3 = f_4 = 75$ mm); DM, dichroic mirror; PMT, photomultiplier tube; SMF, single-mode fiber.

The interaction field is detected by two arms. The first is the phase imaging arm consisting of a lens L_4, a single-mode fiber (with a mode field diameter of ∼4 µm), and a Si avalanche photodetector (APD120A2, Thorlabs), which is not shown in Fig. 1. The second is the fluorescence arm consisting of a dichroic mirror (DM), a fluorescence filter (MF535-22, Thorlabs), a lens (L_3), and a photomultiplier tube (PMT1001/M, Thorlabs). The signals of the two photodetectors are digitalized by an analog-to-digital converter (PCI8514, ART Technology) parallelly. Finally, the raw data is post-processed to retrieve the phase and fluorescence of the sample. The recovered fluorescence and phase images are inherently aligned thanks to single-pixel detection.

4. RESULTS

We experimentally demonstrate phase imaging and simultaneous fluorescence and phase microscopy in this section. The pixel resolution of the result is 128×128, and total number of patterns for each sample is $49,152$. The data acquisition time for each sample is ∼8 minutes, because the RAM of the DMD is only 512 MB with the maximum number of pre-load binary patterns of $5,000$ and we need 10 rounds to load all the patterns. The acquisition time could be reduced to ∼2.5 seconds by replacing the DMD with a larger RAM, such as V7001, ViALUX. We use 6×6 pixel binning of the DMD for maximum illumination intensity at the sample plane, i.e., 768×768 of the DMD pixels are used in the experiment. Note that 2×2 pixel binning is also feasible, we use large pixel binning considering the modulation efficiency and detection sensitivity, because the Lee hologram method has the efficiency of complex field modulation of ∼5% and the intensities of single-point detection and fluorescence detection are relatively low.

4.1 Phase Imaging

The sample used in the phase imaging experiment is etched glass with the depth of a few hundred nanometers. The result of phase imaging is shown in Fig. 2. The sample is three characters forming a numer "100" with lower height. The height of the sample is estimated by the phase difference of the sample, that is

$$h(\vec{r}) = \frac{\lambda}{2\pi\Delta n} \cdot \varphi(\vec{r}), \tag{11}$$

where $\varphi(\vec{r})$ denotes the phase difference induced by the sample, λ is the wavelength of the incident light, that is 488 nm in this experiment, and Δn is the difference of the refractive index between the glass and air, that is 0.4630 in the experiment.

From Fig. 2, we can see that the raw phase of the sample matches well with the background phase and the estimated height is about 1000 nm for the three characters "100", which agrees well with the fact that the etching depth is a few hundred nanometers. All phases here are unwrapped using Goldstein phase unwrapping method.[26] The scale bar in Fig. 2 is 500 µm.

4.2 Simultaneous Fluorescence and Phase Microscopy

We use the quantum dot drop to demonstrate simultaneous fluorescence and phase microscopy. The quantum dot is 20% solution of methylammonium lead bromine ($CH_3NH_3PbBr_3$). We drop the solution on pre-cleaned slide glass to form dots or characters.

The results of simultaneous fluorescence and phase microscopy are shown in Fig. 3. The sample is a drop of quantum dot solution on the slide glass, so only a circle can be seen on the images. It is worth noting that the positions of the circle of both fluorescence and phase images are the same without alignment thanks to single-pixel detection, because the position of the sample in the image is merely determined by relative position between the sample and structured illuminations. The phase of the quantum dot sample remains wrapped because the sample has large phase gradients and the Goldstein phase unwrapping method[26] fails. The scale bar in Fig. 3 is 500 µm.

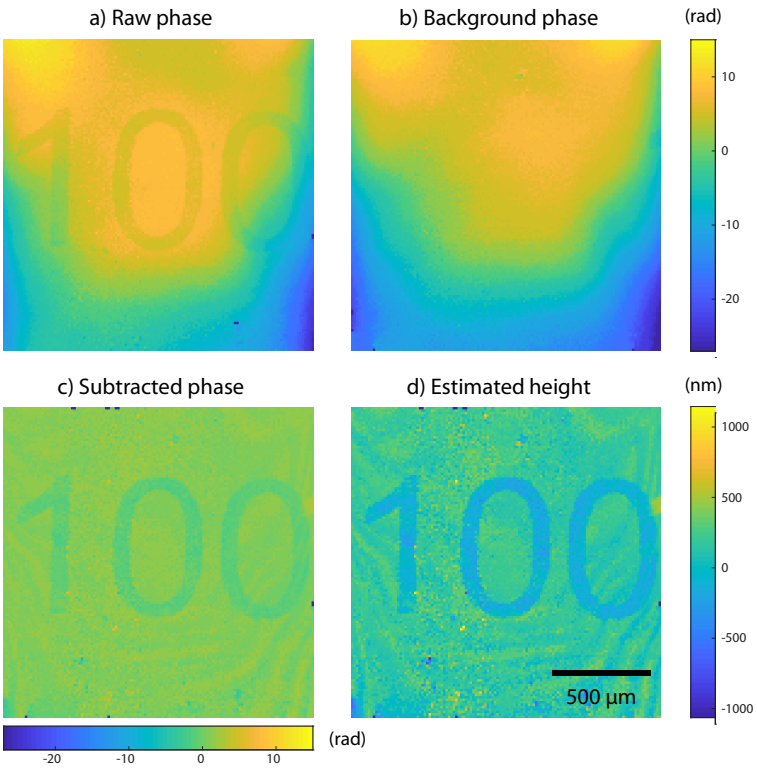

Figure 2. Phase imaging of the etched glass sample. a) Raw phase of the etched glass. b) Background phase of the etched glass. c) Subtracted phase between the raw phase and the background phase displayed at the same colorbar scale. d) Estimated height according to the phase difference induced by the sample. All phases are unwrapped using Goldstein method.[26] Scale bar: 500 µm.

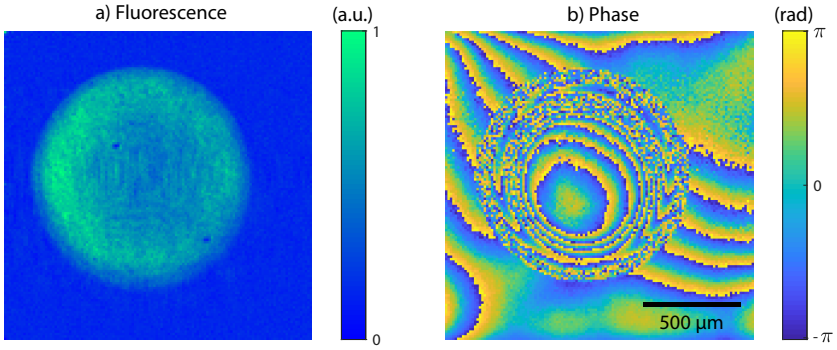

Figure 3. Simultaneous fluorescence and phase microscopy of the quantum dot sample. a) Fluorescence intensity of the quantum dot drop on the slide glass. b) Phase of the quantum dot drop without phase unwrapping because of large phase gradients. Scale bar: 500 µm.

5. CONCLUSIONS AND FUTURE WORK

We report a simultaneous fluorescence and quantitative phase imaging approach using single-pixel detectors. By combining reference-free interferometry with single-pixel detection, we encode the phase and fluorescence of the sample in two detection arms at the same time. This is the first attempt to explore these multimodal microscopy modalities via single-pixel imaging, to the best of our knowledge. This approach is capable of multimodal imaging without expertise demanding alignment of multiple cameras or reduced spatial resolution due to spatial multiplexing. We have demonstrated the phase imaging ability with etched glass and the estimated height

agrees well with the actual etched depth of the sample. Besides, simultaneous fluorescence and phase imaging is also explored by imaging the quantum dot sample, where the fluorescence and phase information agrees with each other. This method can be extended to other wavelengths, where array detectors are expansive or even unavailable, such as infrared imaging,[8,9,21] Terahertz imaging,[27–29] and X-ray imaging.[30,31]

We would further apply this system for observation of biological samples, such as the GFP-labeled *C. elegans*, which contains both fluorescence information (GFP) and phase information (the *C. elegans* is translucent). Current system is not suitable for live cell imaging because it takes minutes to obtain the raw data of a single image. Improvements of the speed of the system could pave the way towards live cell imaging, including using a DMD with a larger RAM to avoid repetitive pattern loading, applying multiplexing strategy to accelerate the spatial light modulation process,[32] and using compressive sensing methods to reduce the sampling rate.[6,24,25]

Moreover, with adddtional single-pixel detectors or a spectrometer, this system could be extended for multi-spectral fluorescence microscopy. Futhermore, we envision that this cost-efficient multimodal system might find broad applications in biomedical science and neuroscience.

ACKNOWLEDGMENTS

The authors thank You Zhou and Liheng Bian for inspiring discussions. The authors would like to share special thanks to Prof. Xing Sheng and Zhao Shi from Department of Electronic Engineering, Tsinghua University for helping prepare the etched glass sample, and Prof. Haizheng Zhong and Linghai Meng from School of Materials Science and Engineering, Beijing Institute of Technology for helping prepare the quantum dot sample. This work was supported by the National Natural Science Foundation of China (No. 61327902, 61722110, 61671265 and 61627804).

REFERENCES

[1] Pawley, J., [*Handbook of Biological Confocal Microscopy*], Springer US, 3rd ed. (2006).
[2] Popescu, G., [*Quantitative phase imaging of cells and tissues*], McGraw-Hill (2011).
[3] Park, Y., Popescu, G., Badizadegan, K., Dasari, R. R., and Feld, M. S., "Diffraction phase and fluorescence microscopy," *Optics Express* **14**(18), 8263–8268 (2006).
[4] Chowdhury, S., Eldridge, W. J., Wax, A., and Izatt, J. A., "Spatial frequency-domain multiplexed microscopy for simultaneous, single-camera, one-shot, fluorescent, and quantitative-phase imaging," *Opt Lett* **40**(21), 4839–42 (2015).
[5] Chowdhury, S., Eldridge, W. J., Wax, A., and Izatt, J. A., "Structured illumination multimodal 3D-resolved quantitative phase and fluorescence sub-diffraction microscopy," *Biomedical Optics Express* **8**(5), 2496 (2017).
[6] Duarte, M. F., Davenport, M. A., Takhar, D., Laska, J. N., Ting, S., Kelly, K. F., and Baraniuk, R. G., "Single-pixel imaging via compressive sampling," *IEEE Signal Processing Magazine* **25**(2), 83–91 (2008).
[7] Sun, B., Edgar, M. P., Bowman, R., Vittert, L. E., Welsh, S., Bowman, A., and Padgett, M. J., "3D computational imaging with single-pixel detectors," *Science* **340**(6134), 844–847 (2013).
[8] Radwell, N., Mitchell, K. J., Gibson, G. M., Edgar, M. P., Bowman, R., and Padgett, M. J., "Single-pixel infrared and visible microscope," *Optica* **1**(5), 285 (2014).
[9] Edgar, M. P., Gibson, G. M., Bowman, R. W., Sun, B., Radwell, N., Mitchell, K. J., Welsh, S. S., and Padgett, M. J., "Simultaneous real-time visible and infrared video with single-pixel detectors," *Sci Rep* **5**, 10669 (2015).
[10] Welsh, S. S., Edgar, M. P., Bowman, R., Jonathan, P., Sun, B., and Padgett, M. J., "Fast full-color computational imaging with single-pixel detectors," *Opt Express* **21**(20), 23068–74 (2013).
[11] Bian, L., Suo, J., Situ, G., Li, Z., Fan, J., Chen, F., and Dai, Q., "Multispectral imaging using a single bucket detector," *Sci Rep* **6**, 24752 (2016).
[12] Wang, Y., Suo, J., Fan, J., and Dai, Q., "Hyperspectral computational ghost imaging via temporal multiplexing," *IEEE Photonics Technology Letters* **28**(3), 288–291 (2016).
[13] Li, Z., Suo, J., Hu, X., Deng, C., Fan, J., and Dai, Q., "Efficient single-pixel multispectral imaging via non-mechanical spatio-spectral modulation," *Sci Rep* **7**, 41435 (2017).

[14] Pian, Q., Yao, R., Sinsuebphon, N., and Intes, X., "Compressive hyperspectral time-resolved wide-field fluorescence lifetime imaging," *Nature Photonics* **11**(7), 411–414 (2017).

[15] Clemente, P., Durán, V., Tajahuerce, E., Torres-Company, V., and Lancis, J., "Single-pixel digital ghost holography," *Physical Review A* **86**(4), 041803 (2012).

[16] Clemente, P., Durán, V., Tajahuerce, E., Andres, P., Climent, V., and Lancis, J., "Compressive holography with a single-pixel detector," *Opt Lett* **38**(14), 2524–7 (2013).

[17] Martínez-León, L., Clemente, P., Mori, Y., Climent, V., Lancis, J., and Tajahuerce, E., "Single-pixel digital holography with phase-encoded illumination," *Optics Express* **25**(5), 4975 (2017).

[18] Lee, W.-H., "III computer-generated holograms: Techniques and applications," *Progress in Optics* **16**, 119–232 (1978).

[19] GonzDuránlez, H., Martínez-León, L., Soldevila, F., Araiza-Esquivel, M., Tajahuerce, E., and Lancis, J., "High-speed single-pixel digital holography," in [*SPIE Optical Metrology*], Ferraro, P., Grilli, S., Ritsch-Marte, M., and Hitzenberger, C. K., eds., **10333**, 103330G, SPIE (2017).

[20] Goorden, S. A., Bertolotti, J., and Mosk, A. P., "Superpixel-based spatial amplitude and phase modulation using a digital micromirror device," *Opt Express* **22**(15), 17999–8009 (2014).

[21] Shin, S., Lee, K., Baek, Y., and Park, Y., "Optical transducer exploiting time-reversal symmetry," *arXiv (preprint)* , 1710.01134 (2017).

[22] Zhang, Z., Ma, X., and Zhong, J., "Single-pixel imaging by means of fourier spectrum acquisition," *Nat Commun* **6**, 6225 (2015).

[23] Zhang, Z., Wang, X., Zheng, G., and Zhong, J., "Hadamard single-pixel imaging versus fourier single-pixel imaging," *Optics Express* **25**(16), 19619–19639 (2017).

[24] Candès, E. J. and Tao, T., "Near-optimal signal recovery from random projections: Universal encoding strategies?," *IEEE Transactions on Information Theory* **52**(12), 5406–5425 (2006).

[25] Candès, E. J., Romberg, J., and Tao, T., "Robust uncertainty principles: exact signal reconstruction from highly incomplete frequency information," *IEEE Transactions on Information Theory* **52**(2), 489–509 (2006).

[26] Goldstein, R. M., Zebker, H. A., and Werner, C. L., "Satellite radar interferometry: Two-dimensional phase unwrapping," *Radio Science* **23**(4), 713–720 (1988).

[27] Watts, C. M., Shrekenhamer, D., Montoya, J., Lipworth, G., Hunt, J., Sleasman, T., Krishna, S., Smith, D. R., and Padilla, W. J., "Terahertz compressive imaging with metamaterial spatial light modulators," *Nature Photonics* **8**(8), 605–609 (2014).

[28] Stantchev, R. I., Sun, B., Hornett, S. M., Hobson, P. A., Gibson, G. M., Padgett, M. J., and Hendry, E., "Noninvasive, near-field Terahertz imaging of hidden objects using a single-pixel detector," *Science Advances* **2**(6), e1600190 (2016).

[29] Stantchev, R. I., Phillips, D. B., Hobson, P., Hornett, S. M., Padgett, M. J., and Hendry, E., "Compressed sensing with near-field THz radiation," *Optica* **4**(8), 989–992 (2017).

[30] Yu, H., Lu, R., Han, S., Xie, H., Du, G., Xiao, T., and Zhu, D., "Fourier-transform ghost imaging with hard X rays," *Physical Review Letters* **117**(11), 113901 (2016).

[31] Pelliccia, D., Rack, A., Scheel, M., Cantelli, V., and Paganin, D. M., "Experimental X-ray ghost imaging," *Physical Review Letters* **117**(11), 113902 (2016).

[32] Wang, Y., Liu, Y., Suo, J., Situ, G., Qiao, C., and Dai, Q., "High speed computational ghost imaging via spatial sweeping," *Sci Rep* **7**, 45325 (2017).